Relation of transport properties to microstructure of implanted $Ni_{1-x}P_x$ alloys

A. Traverse
Centre de Spectrométrie Nucléaire et de Spectrométrie de Masse, Bâtiment 108, Boite Postale No.1, 91406 Orsay, France

E. Paumier
Laboratoire d'Etudes et de Recherches sur les Ratériaux, Institut des Sciences de la Matière et du Rayonnement, Université de Caen, Campus II, 14032 Caen Cédex, France

P. Nédellec, H. Bernas, L. Dumoulin, and J. Chaumont
Centre de Spectrométrie Nucléaire et de Spectrométrie de Masse, Bâtiment 108, Boite Postale No.1, 91406 Orsay, France
(Received 29 June 1987)

We have measured the composition dependence of the resistivity and Hall constants in $Ni_{1-x}P_x$ films prepared by the low-temperature implantation technique. In the concentration range $0 \leq x \leq 0.28$, the system goes from the crystalline (and ferromagnetic) to the amorphous (and paramagnetic) state. A quantitative interpretation of our results is presented, based on previous knowledge of the implanted system's structural properties in the same composition range. This analysis provides new information on the magnetism of amorphous clusters inside the crystalline host.

I. INTRODUCTION

The widely studied $Ni_{1-x}P_x$ alloy is one of the canonical amorphous metal-metalloid systems.[1] Its conduction properties (resistivity and thermoelectric power) have been determined[2] in a rather broad concentration range ($0.15 \leq x \leq 0.25$). Resistivity results on samples prepared via different techniques are in good overall agreement.[3] They were interpreted in the frame of the Faber-Ziman theory.[2]

The magnetic properties of this alloy have also received considerable attention, because they exhibit a transition from the ferromagnetic to the paramagnetic regime as x increases from below to above about 0.18.[1] The Curie temperature typically varies from 633 K in pure Ni to 200 K for amorphous $Ni_{0.85}P_{0.15}$, dropping to 50 K for $Ni_{0.82}P_{0.18}$.[4,5] The magnetization measurements in the paramagnetic state (usually performed on thick samples via the Faraday technique) nearly always revealed the existence of magnetic inhomogeneities.

The purpose of this paper was to study the $Ni_{1-x}P_x$ alloy in a wider concentration range, $0 \leq x \leq 0.28$, where it undergoes two different types of transitions: a structural one from the crystalline to the amorphous state, and a magnetic transition from the ferromagnetic to the paramagnetic state.[1] We have used the low-temperature P-implantation technique in thin Ni films to vary the P content continuously in the range $0 \leq x \leq 0.28$ and have thus established a definite correlation between the microstructure of the alloy, determined in previous work,[6,7] and its resistive and magnetic properties.

Standard magnetic measurements such as the Faraday method are difficult to set up in thin samples; hence, we have used the Hall effect, a technique adapted to the investigation of magnetic properties in thin $Ni_{1-x}P_x$ films, as shown by the pioneering measurement performed by Fléchon and Viard[8] on alloys with low x values ($x = 0.09$ and 0.11). Here, the resistivity and Hall voltage have been measured in pure Ni and $Ni_{1-x}P_x$ films in the range $0 \leq x \leq 0.28$.

Our results are interpreted consistently in terms of the structural modifications in implanted $Ni_{1-x}P_x$ (Ref. 6) in this concentration range. When the amorphous state is reached, our measured transport properties are comparable to those of the corresponding alloy prepared by other techniques.[2] In the paramagnetic state, magnetic inhomogeneities have also been found, as in other samples.[1]

II. THE IMPLANTED $Ni_{1-x}P_x$ MICROSTRUCTURE

The structural modifications under low-temperature P implantation were studied in previous work via the channeling technique[6] and transmission electron microscopy (TEM).[7] The main results are the following. Below $x \sim 0.08$, the system is a random fcc alloy, with a fairly high radiation damage level, Ni atoms being displaced from their sites through ballistic collisions with the incoming P ions. Above $x = 0.08$, amorphization takes place: locally the P concentration is high enough to induce a transition between the crystalline state and an amorphous one over a spatial range of several angstroms. The average local minimum P concentration required for the transition to take place is experimentally determined as $x_c = 0.12$ and the average size of the amorphous clusters is $v_c \sim 400$ atomic volumes. For each x value, the volume fraction α of the target in the amorphous state is estimated from the backscattered He particle yield. Its value against x is plotted in Fig. 1 for a channeling experiment performed at 80 K.[6] At liquid-helium temperature, TEM experiments[7] have also shown the existence of a threshold at $x = 0.08$ for the amorphization process occurrence. As the resistivity of the

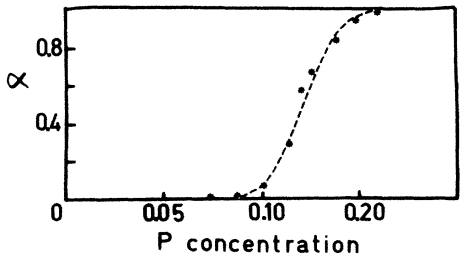

FIG. 1. Amorphous volume fraction α for 80-K P implanted in Ni. From Ref. 6.

amorphous phase is about 4 times higher than that of the crystalline matrix—even when the lattice is disordered—the presence of such amorphous clusters affects the average resistive behavior. Above $x=0.17$, the $Ni_{1-x}P_x$ alloy is homogeneously amorphous. For room-temperature P implantation, the amorphization process is quite different and will not be of interest here.

III. EXPERIMENT

As the Hall voltage in Ni was proved to be thickness dependent, we first checked our measurements against those previously published.[9] For this purpose, pure polycrystalline Ni films of different thicknesses (410–1950 Å) were deposited by electron-gun evaporation, in a vacuum of about 10^{-7} torr, on quartz substrates at room temperature. One Ni film (370 Å) was also deposited on a heated substrate ($T_s \sim 400$ °C) to form larger grains (~ 400 Å instead of ~ 100 Å). The Hall effect and residual resistivities were measured at 4.2 K, that is to say, well below the Curie temperature of pure Ni, in a cryostat equipped with a superconducting magnet delivering a magnetic field of 2 T.

In a second step, the $Ni_{1-x}P_x$ system, prepared by P implantation at 6 K, was studied for $0 \leq x \leq 0.28$. Four Ni films, deposited on a quartz substrate, were mounted in another He cryostat, equipped with a superconducting magnet (4 T). This cryostat could be either coupled to the Orsay implanter, IRMA,[10] or uncoupled from it via a valve during the measurements. The samples are moved vertically from the implantation position to the position in the center of the magnet at a level 12.5 cm higher. To solve the problem of a vertical motion while keeping the samples at 4.2 K, the quartz substrate was fixed on a Cu block held at the extremity of a small He cryostat, moving through a channel inside the main He tank and connected to the latter by a cold valve (see Fig. 2). Its aperture, easily controllable, allows rapid filling or emptying of the inner cryostat, leading to fast temperature cycling. A small liquid-He flow, obtained with the cold valve slightly opened, acts as a cold source which, when balanced by a hot source provided by a heater inside the Cu block, allows very precise temperature stabilization in the range 1.3–80 K. The Cu block can also be rotated in order to bring the samples in a parallel or perpendicular magnetic field; good thermal contact is kept during this motion via stranded copper connected to the inner cryostat. A horizontally mobile diaphragm was positioned in front of the Cu block, with four windows corresponding to dimensions of one, two, three, or four samples. Combining the vertical motion of the inner cryostat and the use of this diaphragm, any of the four samples could be implanted together with one, two, or three other neighboring films. The accuracy of the measurement of the ion implantation fluence was es-

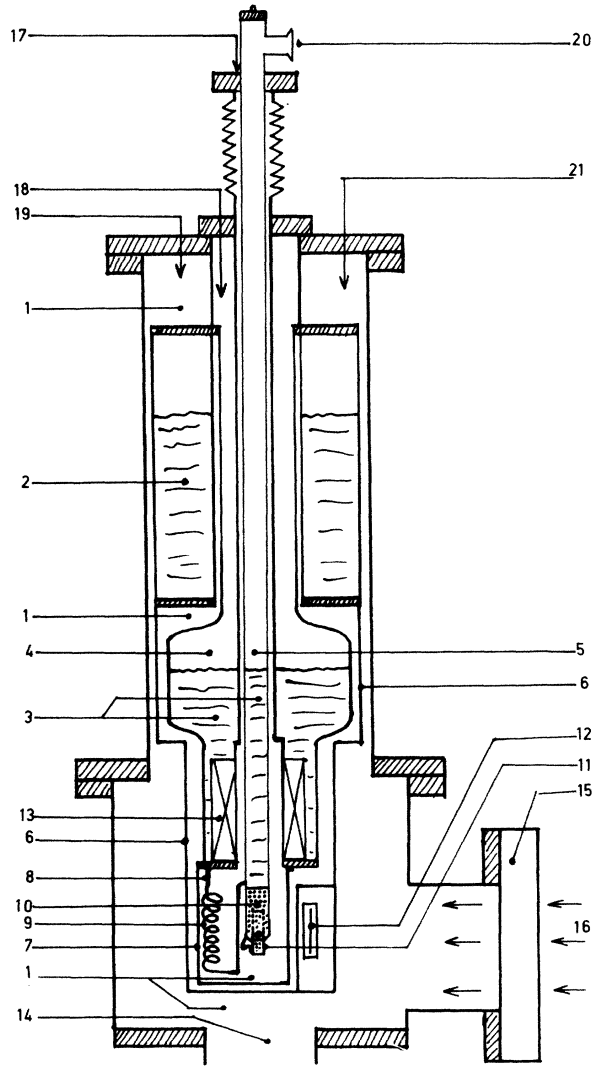

FIG. 2. Scheme of the cryostat equipped with its superconducting magnet which can be coupled to the implanter. 1, vacuum; 2, liquid nitrogen; 3, liquid helium; 4, main liquid-He tank; 5, small inner liquid-He tank; 6, Cu screen at liquid N_2 temperature; 7, Cu screen at liquid-He temperature; 8, cold valve for liquid-He flow; 9, spring capillary for liquid-He flow from 4 to 5; 10, Cu block with a wired heater; 11, rotating sample holder, thermalized by stranded Cu on 10; 12, diaphragm; 13, 4-T magnet; 14, turbomolecular pumping; 15, valve for uncoupling the cryostat from the implanter; 16, ion beam; 17, electrical feedthroughs and rotation control of the sample; 18, electrical feedthroughs of the magnet and liquid-He filling; 19, liquid-N_2 filling and cold valve control; 20, He pumping; and 21, diaphragm control.

timated to be 10%. A typical sequence of operation was the following: cryostat connected to IRMA, samples in the low-level position, P implantation with a different fluence on each sample; cryostat decoupled, samples moved up and rotated to be in a perpendicular magnetic field, measurements on the four samples; cryostat coupled again to IRMA, new implantation with four new fluences; measurements, and so on.

Film thicknesses (550 and 800 Å) and implantation energies were chosen (50–150 keV) in order to obtain rather homogeneous alloys, taking into account the effect of sputtering on the ion distribution profile. Typical P-implanted fluences are about 10^{17} ions cm^{-2}. The P concentration was measured and the homogeneity of the P distribution was checked in the four highly implanted films after annealing up to 300 K, using the Rutherford backscattering technique with the He beam delivered by the implanter. At high concentrations, the P distributions are not affected by annealing up to room temperature.[6] The resistivity was measured at 4.2 K after each implantation step and, using ac measurements, the Hall voltage was followed against the magnetic induction at 4.2 K and in some cases at 80 K.

IV. HALL EFFECT IN Ni AND ITS ALLOYS

The Hall resistivity ρ_H is given by

$$\rho_H = V_H t / I \ , \tag{1}$$

where V_H is the Hall voltage, t the sample thickness, and I the current. An experimental V_H versus B curve, obtained in a magnetic sample such as Ni (shown in Fig. 3 for $x=0.0$) can be described empirically by the following formula in SI units, using the notation of Hurd:[11]

$$\rho_H = (R_0 B + R_S M)\mu_0 \ , \tag{2}$$

where M is the magnetization in A/m, μ_0 the vacuum magnetic permeability, and B the applied induction in T. The ordinary Hall coefficient R_0, expressed in m^3/A s, accounts for the Lorentz force acting on the electrons, while R_S, the spontaneous Hall coefficient expressed in the same units, is a characteristic contribution for magnetic materials. If B is written in terms of the internal magnetic field H_i, Eq. (2) becomes

$$\begin{aligned} B &= (H_i + NM)\mu_0 \ , \\ \rho_H &= (R_0 H_i + R_1 M)\mu_0 \quad \text{with } R_1 = R_0 + R_S \ , \end{aligned} \tag{3}$$

where R_1 is the extraordinary Hall coefficient and N the demagnetization factor, equal to unity in thin films.[12] For low B values, the slope at the origin of ρ_H versus B is R_1.[12] When all the domains are aligned, the spin saturation is reached, the magnetization is M_s, and the Hall voltage is linear versus B with a slope R_0.[11]

In the low-field regime, the normal Hall coefficient R_0 is equal to $1/n^*e$, in a free-electron model, where n^* is the effective number of charges per unit volume.[11] In Ni, R_0 is negative,[13] indicating electronic conduction.

As shown by Hurd,[11] the spontaneous Hall coefficient R_S (negative in Ni) is

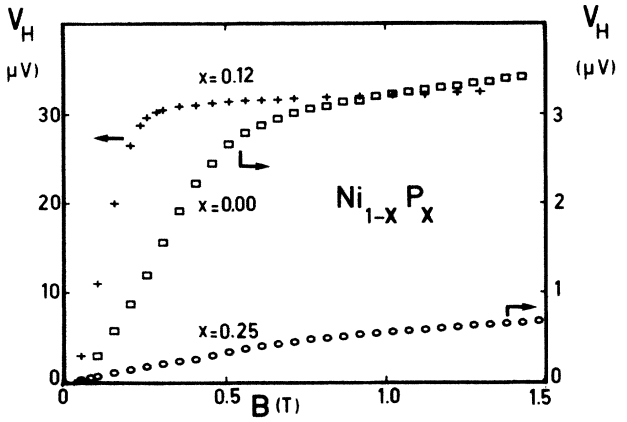

FIG. 3. Hall voltage against the applied induction B measured on $Ni_{1-x}P_x$ films for three x values: $x=0$, $x=0.12$, and $x=0.25$. Note the different vertical scales.

$$R_S \propto \rho_0^2 \sigma_H^{(1)} \ , \tag{4}$$

where $\sigma_H^{(1)}$ only depends on the spin of the system and ρ_0 is its residual resistivity.

Previous Hall-effect measurements on the thin Ni films, performed by Le Bas,[9] had revealed the existence of an easy magnetization axis inducing a remanent magnetization vector in the absence of applied induction, tilted at an angle to the film plane. This affects both the initial slope of the Hall resistivity (the measured quantities R_1 and R_S become R_1' and R_S'), and the saturation magnetization (which is now B_S instead of M_S, B_S being the projection of M_S on the applied field direction). These film effects also depend on evaporation conditions and subsequent annealing treatments.[9]

The magnitude of R_0 is affected by alloying at concentrations high enough to modify the band structure and consequently the number of charges per unit volume.[14] Through ρ_0, R_S is strongly correlated to the disorder in the sample, as experimentally shown in several cases.[14]

In the paramagnetic state, which is reached for $x \sim 0.18$ in $Ni_{1-x}P_x$,[1] the Hall resistivity must be linear with H:

$$\rho_H = (R_0 + R_s \chi) H \ , \tag{5}$$

where χ is the magnetic susceptibility.[11]

V. RESULTS

The values of R_0, R_1', and R_S', equal to $R_1' - R_0$, were found to be negative, in Ni films whatever the P concentration from 0 up to 0.28; hence, in the following we have omitted the negative sign and only presented the absolute values.

A. On pure Ni films

In agreement with the results of Le Bas,[9] our measured average value of B_S is 0.48 T (the bulk value being 0.6 T). Our values of R_1' [typically $(10.39 \pm 1.50) \times 10^{-10}$ m^3/A s for $550 \le t \le 1950$ Å] agree with those

of Ref. 9. We also find an effect of crystallinity since $R_1'(t=410\ \text{Å})=46.27\times10^{-10}\text{m}^3/\text{A s}$, while $R_1'(t=370$ Å, heated substrate) $=10.59\times10^{-10}$ $\text{m}^3/\text{A s}$. By contrast, R_0 does not vary with t and its average value is $R_0=(0.68\pm0.05)\times10^{-10}$ $\text{m}^3/\text{A s}$, in agreement with bulk values.[9] To obtain comparable values for R_1', the thickness of our samples through the whole concentration range was chosen to be at least 500 Å.

B. On P-implanted Ni films

In the range $0.04\leq x\leq0.16$, the Hall voltage qualitatively behaves as in pure Ni, with R_0, R_1', and B_S varying with x. For $x=0.25$ and 0.28 (Fig. 3), the Hall voltage indicates a strong modification of the magnetic character of the alloy. The quantities ρ_0, R_0, and R_1' are plotted versus x in Fig. 4. Experimental uncertainties arise mainly from the sample thickness determination and from the Hall voltage slope measurement; ρ_0 is given $\pm10\%$ and R_0, R_1', R_S', and B_S are given $\pm15\%$.

VI. INTERPRETATION

Consider Fig. 4. Around $x\sim0.08$, both R_0 and ρ_0 change their slopes, while above $x\sim0.18$, R_0 and R_S' display decreasing values. We shall define three concentration ranges: (i) x smaller than 0.08, (ii) an intermediate range $0.08\leq x\leq0.17$, and (iii) x larger than 0.17, in strong correlation with the analysis of the structural properties of $Ni_{1-x}P_x$, as mentioned above.[6] We discuss the behavior of ρ_0, R_0, and R_S' inside each range.

A. Dilute crystalline $Ni_{1-x}P_x$ alloys

In the $0\leq x<0.08$ range, the residual resistivity ρ_0 increases due to disorder resulting from the presence of P ions and of displaced Ni atoms. The roughly linear slope is 2.10 $\mu\Omega$ cm/at. %, that is to say, of the same order of magnitude as the resistivity increase for B in Ni [1.4 $\mu\Omega$ cm/at. % (Ref. 15)] and C in Ni [3.4 $\mu\Omega$ cm/at. % (Ref. 16)] when these impurities are introduced in the matrix by quenching. This shows that the electron scattering process is dominated by the metalloid's presence and not by the displaced Ni atoms.

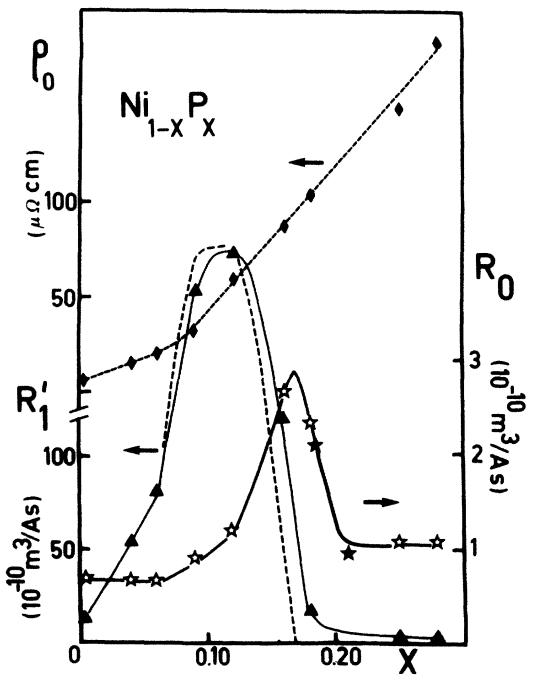

FIG. 4. Residual resistivities ρ_0, normal (R_0) and extraordinary (R_1') Hall coefficients plotted vs x. For $x>0.17$, R_0 values of Ref. 21 (solid stars) are also plotted for comparison. Solid lines are to guide the eye. The dotted line is a calculated variation (see text) for R_S' in the range $0.08<x<0.17$.

The increase in ρ_0 directly affects the variation of R_S'. In Table I, R_S' and ρ_0^2 are directly proportional up to $x\sim0.06$, with a ratio of 0.22 on the average. This is in agreement with Eq. (4), provided that the factor $\sigma_H^{(1)}$ is kept constant: this implies that the magnetic properties of the alloy are not modified, in line with the near constancy of B_S values (see Table I). The constancy of R_0

TABLE I. Residual resistivities ρ_0, spontaneous Hall coefficients R_S', and magnetic induction at saturation, B_S, for $Ni_{1-x}P_x$ samples with $0\leq x\leq0.28$.

Film	ρ_0(4.2 K) ($\mu\Omega$ cm)	B_S (T)	R_S' ($10^{-10}\text{m}^3/\text{A s}$)	R_S'/ρ_0^2
pure Ni	6.8	0.42	11.18	0.24
pure Ni	6.8	0.48	9.62	0.21
pure Ni	6.18	0.50	8.16	0.21
pure Ni	6.43	0.45	9.38	0.23
$Ni_{0.96}P_{0.04}$	15.39	0.44	53.26	0.22
$Ni_{0.94}P_{0.06}$	19.34	0.37	79.84	0.21
$Ni_{0.91}P_{0.09}$	32.35	0.23	186.0	0.18
$Ni_{0.88}P_{0.12}$	59.20	0.20	203.8	0.06
$Ni_{0.84}P_{0.16}$	87.74	0.12	116.3	0.02
$Ni_{0.82}P_{0.18}$	104.8	0.15	23.15	0.02
$Ni_{0.75}P_{0.25}$	150.0	0.37	1.86	
$Ni_{0.71}P_{0.28}$	184.1	0.74	1.54	

suggests that, in this concentration range, our measurement is not sensitive to band-structure modifications of pure Ni due to P allowing.

B. The amorphous concentrated $Ni_{1-x}P_x$ alloys

In the range $x > 0.17$, the sample is completely amorphous. However, increasing the P concentration leads to a resistivity increment, in agreement with previous resistive studies.[2,3]

The Hall voltage (see Fig. 3) no longer displays a clear saturation of the magnetization. As in Ref. 17, we interpret this variation as due to the coexistence of magnetic and nonmagnetic regions in the sample. The B_S increase, up to 0.74 T—higher than the value measured in pure Ni—indicates that these moments are more difficult to saturate, hence less coupled to each other. The similarity of the Hall voltage at 4.2 and 80 K and the presence of hysteresis are in line with magnetic inhomogeneities with a high Curie temperature. Magnetic inhomogeneities,[18] like superparamagnetic particles or giant moment paramagnetic clusters,[19] were also found in $Ni_{1-x}P_x$ or Ni-P-B alloys.[20] Here the system is metallurgically homogeneous, so the observed effect can only be due to statistical Ni clustering with the corresponding appearance of ferromagnetism.

From the linear part of the curve, for B values higher than 1 T, we can deduce R_0 plotted in Fig. 4 against x. Note that the term $R_S\chi$ which appears in Eq. (5) is about 3 orders of magnitude smaller than the measured slope, hence negligible, if we use the value given in Ref. 20 and our R_S value of 25×10^{-10} m^3/A s. After an increase from pure Ni to $Ni_{0.82}P_{0.18}$, R_0 decreases, a surprising feature which has already been found.[21] To our knowledge, no band-structure calculations for these concentrations are actually available to account for this trend.

Between these two extreme ranges where our results on transport properties agree with previous work, lies a region where the amorphization process, well characterized when induced by implantation, takes place.

C. The amorphization region

In the $0.08 \leq x \leq 0.17$ range, there is a rather large R_0 increase, while ρ_0 displays a higher linear slope, and R_S' a maximum value for $x \sim 0.12$. These three variations have to be explained coherently using our knowledge of the alloy microstructure, i.e., amorphous clusters embedded in a disordered matrix.[6] The system is an inhomogeneous mixture, whose transport properties will depend on the volume fraction α of amorphous clusters.

1. Residual resistivity and normal Hall effect

Attempts to provide a quantitative description of the transport properties for heterogeneous media have been developed since the pioneering works of Clausius-Mossoti and Bruggeman.[22] The heterogeneous conductor made up of entities with differing conducting properties (insulating spheres in a metallic matrix, for example) is approximated by an effective medium whose properties are calculated from a macroscopic point of view in the following way. The effective conductivity is a function of the conductivity of each medium (σ_0 and σ_1) and of the volume fraction α of one medium relative to the other. The geometry of the system must be taken into account: in the Bruggeman symmetric theory (BS), clusters of conductivities σ_0 and σ_1 are in contact with each other, while in the Bruggeman asymmetric calculation (BA), spheres of conductivity σ_1 are embedded in a medium whose conductivity is σ_0. See the review given by Landauer.[23] As discussed in the Appendix, we have analyzed our results in the framework of the BS model. In this model, the effective medium theory of Ref. 24 provides us with an effective conductivity $\sigma = f\sigma_0$ where the function f depends on the ratio of the component conductivities and on the volume fraction α. The normal Hall coefficient of the heterogeneous medium depends, in a more complicated way, on the same two variables as well as on the normal Hall coefficients of each component (see the Appendix).

We have compared our resistive and normal Hall coefficient data with theoretical calculations in the frame of this theory. In our system, the α parameter is determined in a completely independent way by the channeling experiments of Ref. 6. The resistivity ρ_0 and the normal Hall coefficient R_{00} of the medium surrounding the amorphous clusters were taken as the resistivity and normal Hall coefficient of the disordered matrix for $x = 0.08$. The resistivity ρ_1 and the normal Hall coefficient R_{01} of the amorphous clusters, taken for $x = 0.17$, are the resistivity and coefficient of the homogeneous amorphous system. Note that the electronic mean free path, in amorphous alloys, is at most two or

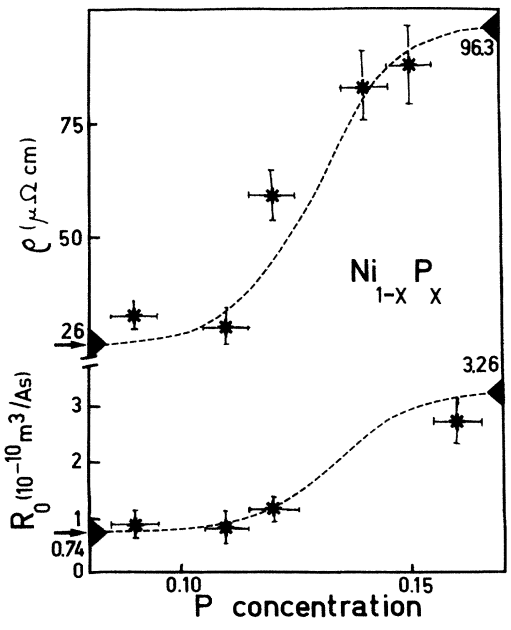

FIG. 5. Comparison between experimental values of ρ and R_0 and those calculated from an effective medium theory. Solid triangles at $x = 0.08$ and 0.17 are values taken for ρ_0, ρ_1 and R_{00}, R_{01}.

three interatomic distances, hence shorter than the dimension of the amorphous cluster ($\sim$400 atomic volumes, hence $\sim$7.5 interatomic distances); so it is possible to define a cluster resistivity. Figure 5 displays the comparison between calculated ρ and R_0 plotted against x and the experimental values. Taking into account the experimental uncertainties and the fact that there are no free parameters, the agreement is quite adequate.

2. *Extraordinary Hall effect*

Within the same picture of amorphous clusters embedded in a disordered matrix, we can also interpret the R_S' behavior. Notice that for $x \geq 0.09$, in Table I, the proportionality between R_S' and ρ_0^2 is no longer observed. Guided by the fact that for $x=0.17$, R_S' reaches a low value, the simplest assumption is that the amorphous clusters are nonmagnetic, while the rest of the matrix is still magnetic. From Eq. (4), R_S' is submitted to a competition between an increase with x due to the ρ_0 increase, and a decrease of $\sigma_H^{(1)}$ due to the nonmagnetic character of the amorphous clusters. The existence of nonmagnetic amorphous clusters is also suggested by the decrease of B_S in this composition range. As shown in Table I, the proportionality coefficient in Eq. (4) is $K=0.21$ for $x<0.08$. We assume (i) that, in this form, Eq. (4) holds in the amorphization range and (ii) that the spin-dependent term $\sigma_H^{(1)}$ is due to the interaction between those Ni spins which are not in the amorphous clusters. This leads to $R_S'=0.21\rho_0^2(1-\alpha)^2$. Values calculated with these very crude assumptions are compared (dotted curve) to the experimental ones in Fig. 4: rather good agreement is found, giving some confidence in our simple model.

It may be surprising that an average local P concentration of 0.12 leads to nonmagnetic clusters, while it is generally admitted that the ferromagnetic to paramagnetic transition occurs for $x \sim 0.18$ in bulk samples. Three explanations may be offered to account for these discrepancies. The amorphization process, as determined in implanted alloys, could be a universal one; hence, the magnetization which is measured in samples prepared by other techniques, instead of coming from the amorphous part of the sample, arises from remaining $Ni_{1-x}P_x$ crystallites, as in our case. But formation of these amorphous clusters in thick quenched samples, for example, could be particularly difficult to observe in the concentration range where the magnetic measurements are performed, typically around $x=0.15$,[1] for which the α value is already near one. Another possibility may be that the reduction of Ni atoms in a cluster induces a decrease of the Curie temperature and spontaneous magnetization.[25] Magnetic properties are also modified by strain in Fe.[25] Here, both dimensional effects due to the small size of the amorphous clusters, and strain effects because of the presence of these clusters in a nonamorphous matrix, can reduce the P concentration required to induce the paramagnetic transition. Lastly, the recently demonstrated[26] difference in the density of states at the Fermi level in implanted amorphous $Ni_{1-x}P_x$ alloys could explain the difference in magnetic properties.

VII. CONCLUSION

Our measurements of the transport properties in crystalline ($x<0.08$) and amorphous ($x>0.17$) P-implanted Ni are in complete agreement with previous results on the resistive and magnetic behavior found in the literature.

New data are presented concerning the intermediate concentration range in which the amorphization process takes place. Assuming the amorphization mechanism derived from previous transmission electron microscopy[7] and channeling experiments,[6] and taking the volume fraction of amorphous clusters thus obtained experimentally, we have established, for the first time, to our knowledge, a direct correlation between the structural and the electronic properties of this alloy. Since (i) the resistivity is sensitive to disorder, (ii) the normal Hall coefficient R_0 depends on the number of electrons per unit volume, and (iii) the spontaneous Hall coefficient R_S' is sensitive to disorder and magnetic state of the sample, the variation of these three quantities with composition were quantitatively connected, without any free parameter, to the amount of amorphous clusters.

Our measurements also bring new insight concerning the amorphous clusters and the totally amorphous alloy. We conclude that the clusters are nonmagnetic with a number of electrons reduced by a factor of $\sim$4, R_0 passing from 0.68 in pure Ni to 2.73×10^{-10} m^3/A s, which requires further band-structure calculations to be explained. The paramagnetic transition in the clusters occurs for $x=0.12$ instead of 0.18, as observed for bulk samples. We have offered two reasons to account for this discrepancy. While the totally amorphous alloy appears to be homogeneous in channeling experiments, the Hall effect detects magnetic inhomogeneities, for $x>0.17$, which may be due to statistical concentration fluctuations. This is not a special feature of the implantation technique, since it was observed in amorphous NiP prepared by different procedures[18,19] and in other amorphous alloys.[20]

Lastly, this work shows the interest of the implantation technique as a way to study the physical properties of a system during structural transformation processes, due to the careful control of composition and disorder.

ACKNOWLEDGMENTS

We thank F. Réthoré and F. Lalu for their assistance during the ion implantation experiments. We are also grateful to P. Purer for his collaboration in the early stages of the experiment.

APPENDIX

Calculations performed either with BA or BS theories, using our experimental values of ρ_0 and ρ_1, lead to σ versus α variations whose differences lie below a few percent, i.e., of the order of the experimental uncertainty. Although the amorphization process occurring in our experimental situation is close to the asymmetric case, we have thus used the BS model for which the conductivity and Hall constant are given in the literature[24] by the following expressions:

$$\sigma = f\sigma_0 ,$$

$$f = 0.25[\gamma + (\gamma^2 + 8\lambda)^{0.5}] ,$$

where λ is the ratio σ_1/σ_0. γ is given by

$$\gamma = 2 - \lambda - 3\alpha(1-\lambda) ,$$

where α is the volume fraction of medium 1. The ordinary Hall constant is given by

$$R_0 = R_{00} f^{-2} \frac{(2f+\lambda)^2(1-\alpha) + (2f+1)^2(\alpha z)}{(2f+\lambda)^2(1-\alpha) + (2f+1)^2\alpha}$$

with $\alpha z = R_{01}\lambda^2 / R_{00}$.

[1] J. Durand, in *Glassy Metals II*, Vol. 53 of *Topics in Applied Physics*, edited by H. J. Güntherodt and H. Beck (Springer-Verlag, Berlin, 1983).

[2] J. P. Carini, S. R. Nagel, L. K. Varga, and T. Schmidt, Phys. Rev. B **27**, 7589 (1983); P. J. Cote, Solid State Commun. **18**, 1311 (1976).

[3] L. Thomé, A. Traverse, and H. Bernas, Phys. Rev. B **28**, 6523 (1983).

[4] D. Pan and D. Turnbull, J. Appl. Phys. **45**, I and II (1974).

[5] A. Berrada, F. Gautier, M. F. Lapierre, B. Loegel, P. Panissod, C. Robert, and J. Beille, Solid State Commun. **21**, 671 (1977).

[6] C. Cohen, A. Benyagoub, H. Bernas, J. Chaumont, L. Thomé, M. Berti, and A. V. Drigo, Phys. Rev. B **31**, 5 (1985).

[7] M. Schack, thèse d'Etat, University of Orsay, 1984.

[8] J. Fléchon and M. Viard, C. R. Acad. Sci. **270**, 84 (1970); **270**, 556 (1970).

[9] J. Le Bas, Thin Solid Films **10**, 429 (1972); **10**, 437 (1972).

[10] J. Chaumont, F. Lalu, M. Salomé, A. M. Lamoise, and H. Bernas, Nucl. Instrum. Methods **189**, 193 (1981).

[11] C. M. Hurd, *The Hall Effect in Metal and Alloys* (Plenum, New York, 1972).

[12] R. C. O'Handley, in *The Hall Effect and Its Applications*, edited by C. L. Chien and C. R. Westgate (Plenum, New York, 1980), p. 417.

[13] L. Berger and G. Bergmann, in *The Hall Effect and Its Applications*, Ref. 12, p. 55.

[14] T. R. McGuire, R. J. Gambino, and R. C. O'Handley, in *The Hall Effect and Its Applications*, Ref. 12, p. 137.

[15] M. C. Cadeville and C. Lerner, Philos. Mag. **33**, 801 (1976).

[16] M. C. Cadeville, C. Lerner, and J. M. Friedt, Physica B + C **86-88B**, 432 (1977).

[17] J. Ivkov, Z. Marohnic, E. Babič, M. Miljak, and H. H. Liebermann, J. Phys. F **13**, 2137 (1983).

[18] K. Iida, J. Magn. Magn. Mater. **35**, 226 (1983).

[19] I. Bakonyi, L. K. Varga, A. Lovas, E. Toth-Kadar, and A. Solyóm, J. Magn. Magn. Mater. **50**, 111 (1985).

[20] A. Anamou and J. Durand, Commun. Phys. **1**, 191 (1976).

[21] S. W. McKnight and A. K. Ibrahim, J. Non-Cryst. Solids **61-62**, 1301 (1984).

[22] D. A. G. Bruggeman, Ann. Phys. (Leipzig) **29**, 160 (1937).

[23] R. Landauer, in *Electric Transport and Optical Properties of Inhomogeneous Media (Ohio State University, 1977)*, Proceedings of the First Conference on the Electrical Transport and Optical Properties of Inhomogeneous Media, AIP Conf. Proc. No. 40, edited by J. C. Garland and D. P. Tanner (AIP, New York, 1978), p. 2.

[24] M. H. Cohen and J. Jortner, Phys. Rev. Lett. **30**, 696 (1973).

[25] U. Gradmann, R. Bergholz, and E. Bergter, Thin Solid Films **126**, 107 (1985); J. P. Renard and P. Beauvillain, Phys. Scr. (to be published).

[26] E. Belin, A. Traverse, A. Szász, and F. Machizaud, J. Phys. F **17**, 1913 (1987).